J|A|C|S ARTICLES

Published on Web 07/20/2009

Multilength-Scale Chemical Patterning of Self-Assembled Monolayers by Spatially Controlled Plasma Exposure: Nanometer to Centimeter Range

Meng-Hsien Lin,[†] Chi-Fan Chen,[†] Hung-Wei Shiu,[‡,§] Chia-Hao Chen,[§] and Shangjr Gwo*[,†,‡]

Institute of Nanoengineering and Microsystems, Department of Physics, National Tsing-Hua University, Hsinchu 30013, Taiwan, and National Synchrotron Radiation Research Center (NSRRC), Hsinchu 30076, Taiwan

Received March 2, 2009; E-mail: gwo@phys.nthu.edu.tw

Abstract: We present a generic and efficient chemical patterning method based on local plasma-induced conversion of surface functional groups on self-assembled monolayers (SAMs). Here, spatially controlled plasma exposure is realized by elastomeric poly(dimethylsiloxane) (PDMS) contact masks or channel stamps with feature sizes ranging from nanometer, micrometer, to centimeter. This chemical conversion method has been comprehensively characterized by a set of techniques, including contact angle measurements, X-ray photoelectron spectroscopy (XPS), scanning photoelectron microscopy (SPEM), scanning electron microscopy (SEM), and scanning Kelvin probe microscopy (SKPM). In particular, XPS and SPEM can be used to distinguish regions of different surface functionalities and elucidate the mechanism of plasma-induced chemical conversion. In the case of an octadecyltrichlorosilane (OTS) monolayer, we show that exposure to low-power air plasma causes hydroxylation and oxidation of the methyl terminal group on an OTS-covered Si surface and generates polar functional groups such as hydroxyl, aldehylde, and carboxyl groups, which can allow subsequent grafting of dissimilar SAMs and adsorption of colloid nanoparticles onto the patterned areas with an achievable resolution down to the 50 nm range.

Introduction

One of the key challenges for implementing widespread applications based on nanotechnology is reliable large-scale integration of single nanoscale objects into functional devices and structures.[1−4] An attractive nanoassembly strategy should allow a large number of hierarchical and multilength-scale organization steps to interface nanoscopic devices and structures with the macroscopic world. Chemical patterning of self-assembled monolayers (SAMs) with designated surface features is a promising technique for achieving these goals.[5−7] In the past decade, several SAM patterning approaches have been demonstrated by means of photolithography,[8−14] controlled exposure to energetic particle beams (electrons, ions, etc.),[15−17] scanning probe microscopy,[18−20] and stamp-based soft lithography.[21] It has also been shown that patterned SAMs can be used as templates for selective adsorption or nucleation of various molecules,[10−13,16,18,19] proteins,[22−24] cells,[22] colloidal

[†] Institute of Nanoengineering and Microsystems, National Tsing-Hua University.

[‡] Department of Physics, National Tsing-Hua University.

[§] National Synchrotron Radiation Research Center.

(1) (a) Huang, Y.; Lieber, C. M. *Pure Appl. Chem.* **2004**, *76*, 2051. (b) Lu, W.; Lieber, C. M. *Nat. Mater.* **2007**, *6*, 841.
(2) (a) Wong, S.; Kitaev, V.; Ozin, G. A. *J. Am. Chem. Soc.* **2003**, *125*, 15589. (b) Ozin, G. A.; Arsenault, A. C. *Nanochemistry: A Chemcal Approach to Nanomaterials*; The Royal Society of Chemistry: Cambridge, U.K, 2005.
(3) (a) Tao, A. R.; Huang, J. X.; Yang, P. D. *Acc. Chem. Res.* **2008**, *41*, 1662. (b) Tao, A. R.; Sinsermsuksakul, P.; Yang, P. D. *Nat. Nanotechnol.* **2007**, *2*, 435.
(4) Chen, C.-F.; Tzeng, S.-D.; Chen, H.-Y.; Lin, K.-J.; Gwo, S. *J. Am. Chem. Soc.* **2008**, *130*, 824.
(5) (a) Xia, Y.; Whitesides, G. M. *Annu. Rev. Mater. Sci.* **1998**, *28*, 153. (b) Xia, Y.; Whitesides, G. M. *Angew. Chem., Int. Ed.* **1998**, *37*, 550.
(6) Smith, R. K.; Lewis, P. A.; Weiss, P. S. *Prog. Surf. Sci.* **2004**, *75*, 1.
(7) Gates, B. D.; Xu, Q.; Stewart, M.; Ryan, D.; Willson, C. G.; Whitesides, G. M. *Chem. Rev.* **2005**, *105*, 1171.
(8) Tarlov, M. J.; Burgess, D. R. F.; Gillen, G. *J. Am. Chem. Soc.* **1993**, *115*, 5305.
(9) Dressick, W. J.; Calvert, J. M. *Jpn. J. Appl. Phys.* **1993**, *32*, 5829.
(10) Friebel, S.; Aizenberg, J.; Abad, S.; Wiltzius, P. *Appl. Phys. Lett.* **2000**, *77*, 2406.
(11) del Campo, A.; Boos, D.; Spiess, H. W.; Jonas, U. *Angew. Chem., Int. Ed.* **2005**, *44*, 4707.
(12) Sugimura, H.; Hong, L.; Lee, K.-H. *Jpn. J. Appl. Phys.* **2005**, *44*, 5185.
(13) Anderson, M. E.; Srinivasan, C.; Hohman, J. N.; Carter, E. M.; Horn, M. W.; Weiss, P. S. *Adv. Mater.* **2006**, *18*, 3258.
(14) Kim, Y.-J.; Lee, K.-H.; Sano, H.; Han, J.; Ichii, T.; Murase, K.; Sugimura, H. *Jpn. J. Appl. Phys.* **2008**, *47*, 307.
(15) Lercel, M. J.; Craighead, H. G.; Parikh, K.; Seshadri, K.; Allara, D. L. *Appl. Phys. Lett.* **1996**, *68*, 1504.
(16) Gölzhäuser, A.; Eck, W.; Geyer, W.; Stadler, V.; Weimann, T.; Hinze, P.; Grunze, M. *Adv. Mater.* **2001**, *13*, 806.
(17) Klinov, D.; Atlasov, K.; Kotlyar, A.; Dwir, B.; Kapon, E. *Nano Lett.* **2007**, *7*, 3583.
(18) (a) Sugimura, H.; Nakagiri, N. *J. Am. Chem. Soc.* **1997**, *119*, 9226–9229. (b) Sugimura, H.; Hanji, T.; Hayashi, K.; Takai, O. *Adv. Mater.* **2002**, *14*, 524.
(19) (a) Maoz, R.; Cohen, S. R.; Sagiv, J. *Adv. Mater.* **1999**, *11*, 55. (b) Hoeppener, S.; Maoz, R.; Cohen, S. R.; Chi, L.; Fuchs, H.; Sagiv, J. *Adv. Mater.* **2002**, *14*, 1036.
(20) Fresco, Z. M.; Fréchet, J. M. J. *J. Am. Chem. Soc.* **2005**, *127*, 8302.
(21) Kumar, A.; Whitesides, G. M. *Appl. Phys. Lett.* **1993**, *63*, 2002.
(22) Mrksich, M.; Whitesides, G. M. *Annu. Rev. Biophys. Biomol. Struct.* **1996**, *25*, 55.

10.1021/ja901619h CCC: $40.75

particles,[20,25−30] inorganic/organic crystals,[31−33] and metals.[34] Among these techniques, the soft lithographic method (parallel process) using an elastomeric stamp is one of the most versatile approaches, which can satisfy simultaneously the needs for scalability, high throughput, and low cost.[5] On the other hand, local chemical conversion of organosilane SAMs using the scanning probe technique (serial process)[18,19] can offer the highest spatial resolution as well as possibilities of creating chemical templates for hierarchical self-assembly.[27] The present work was inspired by these approaches. By combining their advantages, the method reported here could open up a new way for hierarchical and multilength-scale self-assembly of functional nanoscale devices and structures.

At present, the field of elastomeric-stamp-based soft lithography is quite diverse and includes many pioneering variations.[5,7,35−41] Among them, microcontact printing (μCP),[21] micromolding in capillaries (MIMIC),[5,35] and microfluidic networks (μFN)[36−39] are the most representative ones. To date, soft lithographic methods are mainly applied for microscale patterning, while nanoscale patterning and hierarchical processing (multilength-scale from nm to cm range, sequential steps) are still the main issues in soft lithography. For example, the major concerns of the μCP method are the fidelity of pattern transfer, uniformity of large-area processing, and possibility of hierarchical structures.[42] Most of these concerns are related to the transferring of "ink" to the surface during the conformal contact between the patterned sample and the stamp, which is prone to stamp deformation and lateral diffusion of the ink. Although μCP patterning with sub-100-nm resolution is feasible, most of the routinely generated μCP patterns have feature sizes in the micrometer range.

Regarding the other methods in soft lithography, a cited critical drawback of MIMIC and μFN techniques using viscous fluids is the intrinsic slowness in patterning, which limits its use for large-area applications.[40] To overcome this difficulty, Langowski et al. proposed the channel-mediated plasma modification for polymer substrates.[40] Other low-viscosity flow systems such as direct deposition of an SAM pattern on the substrate using microchannel-flowed silane vapor have also been applied for overcoming this problem.[41] However, although these processes reduce the processing time and allow for large-area patterning, they can only be applied for microscale patterning.[40,41] The main issues are related to the strong interaction of plasma with the exposed surfaces and boundary effects in micro- or nanochannels, which can limit the achievable resolution. In this work, we show that the SAM-based self-limiting surface modification is vitally important for achieving the goals for nanoscale and hierarchical processing. Here, to enhance the applicability of soft lithography, we report an "ink"-free soft lithographic method based on plasma-induced, self-limiting chemical modification of organosilane SAMs via poly(dimethylsiloxane) (PDMS) stamp-controlled plasma exposure. Using this approach, we can achieve SAM patterning in the nanometer to centimeter dimension range. Additionally, we demonstrate that this patterning technique can be applied to create versatile surface templates for site-selective grafting of dissimilar SAMs and adsorption of colloidal nanoparticles.

To achieve site-specific chemical modification and large-area patterning, we utilized PDMS elastomeric stamps fabricated by both photolithography and electron-beam lithography (EBL) as contact masks or channel stamps. By conformally contacting the PDMS stamps with surfaces terminated by organosilane SAMs, we can realize controlled exposure or the flow of low-power air plasma on the patterned areas of predeposited organosilane SAMs. The patterning resolution can reach a spatial resolution of 50 nm when EBL-fabricated stamps are used. In this study, we have also clarified the nature of plasma-induced chemical modification. The technique of synchrotron-based X-ray photoelectron spectroscopy (XPS) was applied to confirm the conversion of the surface methyl group ($-CH_3$) into polar functional groups such as a carboxyl ($-COOH$), aldehylde ($-CHO$), and hydroxyl ($C-OH$) group, which can allow subsequent grafting of dissimilar SAMs onto the patterned areas. Moreover, by using field-emission scanning electron microscopy (FE-SEM), scanning Kelvin probe microscopy (SKPM), and synchrotron-based scanning photoemission microscopy (SPEM), we have performed chemical mapping of different functional groups on the plasma-modified surface. Using the technique of SKPM, the surface potential changes are quantitatively measured at the surfaces of plasma-modified regions, dissimilar SAMs, and nanoparticle-adsorbed regions. By comparing all the microscopic results (SEM, SKPM, SPEM), we find that plasma-based pattern transfer using PDMS channel stamps is of high fidelity in terms of chemical conversion and lateral distribution of functional groups on the patterned surfaces.

Experimental Section

The schematic representation of process flow for selective surface chemical modification and controlled self-assembly based on microchannel-flowed plasma (μCFP) is shown in Scheme 1. Other experimental details are described herein.

Fabrication of PDMS Micro- and Nanochannel Stamps. The PDMS stamps were made by pouring a mixture of base and curing

(23) Turchanin, A.; Tinazli, A.; El-Desawy, M.; Groβmann, H.; Schnietz, M.; Solak, H. H.; Tampé, R.; Gölzhäuser, A. *Adv. Mater.* **2008**, *20*, 471.
(24) Ludden, M. J. W.; Li, X.; Greve, J.; van. Amerongen, A.; Escalante, M.; Subramaniam, V.; Reinhoudt, D. N.; Huskens, J. *J. Am. Chem. Soc.* **2008**, *130*, 6964.
(25) Aizenberg, J.; Braun, P. V.; Wiltzius, P. *Phys. Rev. Lett.* **2000**, *84*, 2997.
(26) Jonas, U.; del Campo, A.; Krüger, C.; Glasser, G.; Boos, D. *Proc. Natl. Acad. Sci., U.S.A.* **2002**, *99*, 5034.
(27) Liu, S.; Maoz, R.; Sagiv, J. *Nano Lett.* **2004**, *4*, 845.
(28) Maury, P.; Escalante, M.; Reinhoudt, D. N.; Huskens, J. *Adv. Mater.* **2005**, *17*, 2718.
(29) Chen, C.-F.; Tzeng, S.-D.; Lin, M.-H.; Gwo, S. *Langmuir* **2006**, *22*, 7819.
(30) (a) Ma, L.-C.; Subramanian, R.; Huang, H.-W.; Ray, V.; Kim, C.-U.; Koh, S. J. *Nano Lett.* **2007**, *7*, 439. (b) Huang, H.-W.; Bhadrachalam, P.; Ray, V.; Koh, S. J. *Appl. Phys. Lett.* **2008**, *93*, 073110.
(31) Qin, D.; Xia, Y.; Xu, B.; Yang, H.; Zhu, C.; Whitesides, G. M. *Adv. Mater.* **1999**, *11*, 1433.
(32) (a) Aizenberg, J.; Black, A. J.; Whitesides, G. M. *Nature* **1999**, *398*, 495. (b) Aizenberg, J.; Black, A. J.; Whitesides, G. M. *J. Am. Chem. Soc.* **1999**, *121*, 4500.
(33) (a) Briseno, A. L.; Roberts, M.; Ling, M.-M.; Moon, H.; Nemanik, E. J.; Bao, Z. *J. Am. Chem. Soc.* **2006**, *128*, 3880. (b) Briseno, A. L.; Mannsfeld, S. C. B.; Ling, M. M.; Liu, S.; Tseng, R. J.; Reese, C.; Roberts, M. E.; Yang, Y.; Wudl, F.; Bao, Z. *Nature* **2006**, *444*, 913.
(34) Zhou, C.; Nagy, G.; Walker, A. V. *J. Am. Chem. Soc.* **2005**, *127*, 12160.
(35) Kim, E.; Xia, Y.; Whitesides, G. M. *Nature* **1995**, *376*, 581–584.
(36) Delamarche, E.; Bernard, A.; Schmid, H.; Bietsch, A.; Michel, B.; Biebuyck, H. *Science* **1997**, *276*, 779–781.
(37) Delamarche, E.; Bernard, A.; Schmid, H.; Bietsch, A.; Michel, B.; Biebuyck, H. *J. Am. Chem. Soc.* **1998**, *120*, 500–508.
(38) Kenis, P. J. A.; Ismagilov, R. F.; Whitesides, G. M. *Science* **1999**, *285*, 83–85.
(39) Kenis, P. J. A.; Ismagilov, R. F.; Takayama, S.; Whitesides, G. M.; Li, S.; White, H. S. *Acc. Chem. Res.* **2000**, *33*, 841–847.
(40) Langowski, B. A.; Uhrich, K. E. *Langmuir* **2005**, *21*, 10509–10514.
(41) Julthongpiput, D.; Fasolka, M. J.; Zhang, W. H.; Nguyen, T.; Amis, E. J. *Nano Lett.* **2005**, *5*, 1535–1540.
(42) Sharpe, R. B. A.; Burdinski, D.; Huskens, J.; Zandvliet, H. J. W.; Reinhoudt, D. N.; Poelsema, B. *J. Am. Chem. Soc.* **2005**, *127*, 10344.

Scheme 1. Schematic Illustration (Not to Scale) of Selective Surface Chemical Modification and Controlled Self-Assembly Based on Microchannel-Flowed Plasma (μCFP)[a]

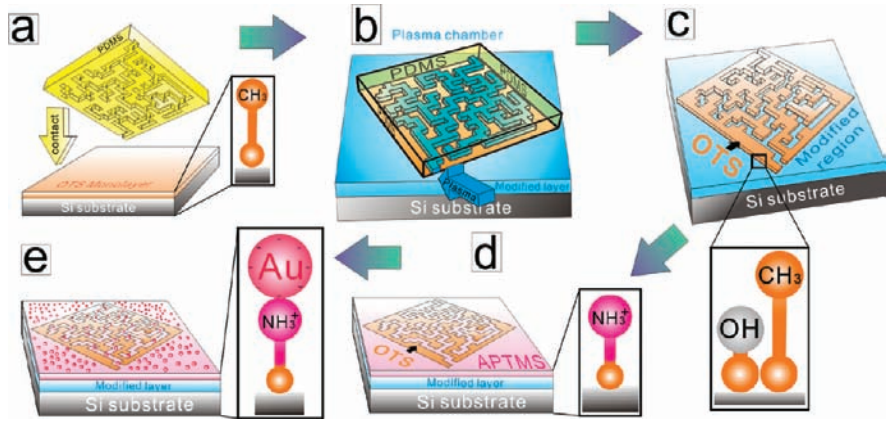

[a] (a) First, the PDMS channel stamp is in conformal contact with a Si substrate covered by an OTS monolayer with the terminal methyl group ($-CH_3$). (b) Local conversion of the terminal group occurs on the OTS monolayer region which is exposed to air plasma (the region within the channel). (c) The terminal group is now converted to polar surface groups such as $-OH$, $-CHO$, and $-COOH$ on the surface region exposed by μCFP, while the terminal functional group remains as the methyl group on the surface region in contact with PDMS. (d) The modified region can be used to selectively graft the second layer (APTMS). (e) The region covered by APTMS can be utilized to adsorb the negatively charged Au nanoparticles.

agent (10:1 w/w) of Sylgard 184 silicone elastomer (Dow Corning) onto patterned molds and curing at 100 °C for 30 min. In this work, three types of μCFP molds were prepared for fabricating PDMS stamps, which have feature sizes ranging from micrometer-, submicrometer-, to nanometer-scale. To prepare molds with micrometer-scale resolution, we utilized a photolithographic process using an SU-8 photoresist (MicroChem, product no. SU-8 2035), which was first spun onto a Si(111) wafer. We then exposed the SU8-coated Si wafer using a UV light source at 365 nm. The thickness of the SU-8 mold is 30 μm, and their line widths range from 5 to 20 μm. For the fabrication of the mold with submicrometer-scale features, we used EBL (electron gun voltage 20 kV, exposure dose: $\sim$150 μC/cm^2) to write resist patterns on poly(methyl methacrylate) (PMMA) with a thickness of 100 nm. After PMMA resist development, the Si mold was obtained by using a reactive ion-etching (RIE) instrument (Oxford Instruments, Plasmalab 80 Plus) with SF_6/O_2 plasma (flow rate: 30/6 sccm, 150 mTorr) at 225 W RF power for 1 min. The thickness of RIE-etched Si molds is 1 μm, and the surface protrusion features, which correspond to the PDMS channel width after pattern replication, are limited by the isotropic RIE step to 600 nm. Finally, for the fabrication of nanoscale PMMA molds, we utilized the cross-linked PMMA as a high-resolution negative resist.[43] The cross-linked PMMA nanostructures were created by a high dose of electron exposure ($\sim$4 mC/cm^2) on a 500-nm-thick PMMA resist using an electron beam operating at 28 kV. The patterned PMMA films were used directly as molds for replicating PDMS stamps. Using this technique, which requires no RIE step, the achievable protrusion feature size in the PMMA mold is on the order of 40 nm, and the corresponding PDMS channel width is 50 nm.

Adsorption of Octadecyltrichlorosilane (OTS) Monolayer on Si Wafer. Octadecyltrichlorosilane [OTS, $H_3C(CH_2)_{17}SiCl_3$] was purchased from Aldrich (product no. 104817). Initially, a 3-in. Si (111) wafer is cleaned by acetone, ethanol, and deionized water. Then, the Si wafer was activated by air plasma (XEI Scientific) at 0.6 Torr and 12 W RF power for 10 min. We immersed the activated wafer into a 0.5 mM OTS/toluene solution for 2 min. Under this condition, a complete OTS monolayer can be formed onto the Si substrate.

Plasma-Induced Surface Chemical Modification. The PDMS channel stamp was first brought into contact with the OTS-overed Si sample. A conformal contact can be readily formed without applying pressure because of the elastomeric nature of PDMS stamp. For the plasma treatment, the sample was loaded in a vacuum chamber equipped with an RF plasma system (XEI Scientific) and a dry vacuum pump. The required air plasma was generated under the conditions of 0.6 Torr (gas source: ambient air) and 12 W RF power. The low-power air plasma used in this process can create active oxygen species for surface modification. Local conversion of the terminal function group occurs on the OTS monolayer region which is exposed to the air plasma.

Grafting of 3-Aminopropyltrimethoxysilane (APTMS) Layer. The selectively modified OTS/Si sample was immersed into a 97% 3-aminopropyltrimethoxysilane solution [APTMS, $H_2N(CH_2)_3Si(OCH_3)_3$, Aldrich, product no. 281778] for 24 h. As a result, the locally modified OTS regions could be grafted with a monolayer of APTMS while the unmodified OTS regions remain with the original surface characteristics.

Adsorption of Gold Nanoparticles (AuNPs). We immersed the APTMS-grafted sample into a gold colloidal solution (Sigma, product no. G1527, ca. 10 nm mean particle size) for 30 min. When the APTMS-grafted sample is immersed into the gold colloidal solution, the APTMS terminal functional group is protonated in the suspension used here (pH 6.25). Therefore, the APTMS-grafted region could selectively adsorb the negatively charged AuNPs.

Field-Emission Scanning Electron Microscopy (FE-SEM). The patterned sample surfaces were imaged with a field-emission scanning electron microscope (Zeiss, Ultra 55).

X-ray Photoelectron Spectroscopy (XPS) and Scanning Photoelectron Microscopy (SPEM). The synchrotron-based microscopy experiments were carried out at an SPEM end station and a spectroscopy end station, which are located at the 09A1 and 09A2 beamlines of the National Synchrotron Radiation Research Center (NSRRC), Hsinchu, Taiwan. The SPEM system is equipped with Fresnel zone plate optics to focus the monochromatic soft X-ray. The beam size at the sample surface under optimized conditions is $\sim$100$-$200 nm, which determines the ultimate spatial resolution of the system. The microscopic images were formed by collecting a characteristic core-level photoelectron signal while raster-scanning the sample relative to the focused soft X-ray beam.[44] The imaging contrast reflects the intensity of the collected photoelectron signal.

(43) Zailer, I.; Frost, J. E. F.; Chabasseur-Molyneux, V.; Ford, C. J. B.; Pepper, M. *Semicond. Sci. Technol.* **1996**, *11*, 1235.

(44) (a) Klauser, R.; Hong, I.-H.; Su, H.-J.; Chen, T. T.; Gwo, S.; Wang, S.-C.; Chuang, T. J.; Gritsenko, V. A. *Appl. Phys. Lett.* **2001**, *79*, 3143. (b) Klauser, R.; Hong, I.-H.; Lee, T.-H.; Yin, G.-C.; Wei, D.-H.; Tsang, K.-L.; Chuang, T. J.; Wang, S.-C.; Gwo, S.; Zharnikov, M.; Liao, J.-D. *Surf. Rev. Lett.* **2002**, *9*, 213.

In such a way, a two-dimensional distribution of a chosen chemical binding state can be mapped. The photon energy used in this study for SPEM was 550 eV, while for the XPS measurements the photon energy was 350 eV.

Atomic Force Microscopy (AFM) and Scanning Kelvin Probe Microscopy (SKPM). AFM and SKPM imaging was performed with a high-vacuum scanning probe microscope (Seiko Instruments, SPA-300HV). The SKPM probe (MikroMasch, CSC37/Cr-Au) has a resonant frequency of 30 kHz and a force constant of 0.35 N/m. In the noncontact imaging mode, an ac voltage of 3 V at a frequency of 28 kHz was applied between the conducting probe tip and the sample to acquire the SKPM images.

Results and Discussion

The "ink-free" soft lithographic method reported here is based on plasma-induced modification of SAM functional groups.[45,46] Plasma cleaning is a commonly used practice to clean or activate sample surfaces for electron microscopy or deposition of functional components. Recently, this technique has also been applied for surface modification. Furthermore, related surface patterning techniques using stamps[40,47] or microplasmas jets[48] have been demonstrated for polymer and silanized glass surfaces, respectively. In this work, the spatially controlled plasma exposure is realized by utilizing the eleastomeric properties of PDMS stamps to form exposure windows or micro- and nanochannels on the patterned surface predeposited with an OTS SAM. By combining several kinds of PDMS stamps, we can achieve multilength scale chemical lithography with versatile patterning capabilities. In typical μCP techniques, a PDMS stamp with a relief structure is brought into conformal contact with a substrate to transfer the relief pattern from the stamp to the substrate via "ink" materials on the relief structure. Recently, Lahav and co-workers showed that, instead of the protrusion part in the relief structure, the depression region can be used to form microfluidic channels, and this approach has been adopted for in-plane surface modification in the liquid phase via ionic exchange reactions.[49] Langowski et al. have also shown that PDMS channel stamps can be used for patterning biomolecular templates on polymer surfaces using oxygen plasma.[47] In both cases, surface modification was performed directly with the exposed polymer surfaces within the microchannels. Here, we introduce a simple and efficient microchannel-flowed plasma (μCFP) process for chemical patterning of organosilane SAMs. We use both micro- and nanochannels which are embossed in PDMS stamps to demonstrate that complex and ultrahigh-resolution (down to the 50 nm range) chemical patterning can be achieved in the μCFP process. It is important to note that the predeposited OTS SAM is crucial to achieve nanoscale resolution and a hierarchical processing capability due to its self-limiting nature while interacting with the plasma. In the following, we will elucidate the plasma-induced conversion mechanism. Detailed comparison with the cases without the surface coverage by a self-limiting SAM is provided in the Supporting Information.

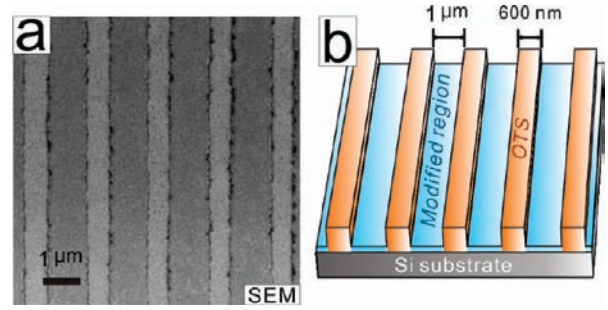

Figure 1. Submicrometer OTS structure fabricated by μCFP process. (a) FE-SEM image of a patterned OTS surface using an EBL-prepared Si mold. The darker regions correspond to the plasma-modified regions, while the brighter regions are the unmodified OTS-covered surface, which was contacted by the PDMS stamp. (b) Schematic illustration.

Multilength-Scale Chemical Patterning of OTS SAMs. As for the chemical patterning on the microscopic scales, Figure 1 shows an FE-SEM image of a patterned OTS surface using a submicrometer-scale PDMS microchannel stamp. FE-SEM has been known to be an effective microscopic approach to resolve the chemically patterned surface due to the sensitivity of secondary electron emission for determining the functional difference in the functional groups as well as other details such as alkyl chain length and extent of molecular ordering.[50,51] Therefore, the imaging contrast revealed by FE-SEM can be used as an easy, qualitative characterization of SAM patterning.

In Figure 2, we demonstrate the state-of-the-art spatial resolution which has been achieved using the present μCFP approach. Figure 2a shows an FE-SEM image of a hardened PMMA grating structure fabricated by EBL with a 40-nm line width. This structure was used directly without further processing as a mold to replicate nanoscale PDMS channel stamps. In this figure, we also show the patterned OTS surface using a nanochannel PDMS stamp replicated from this PMMA mold [Figure 2b], and Figure 2c shows the result after selective grafting of APTMS and adsorption of 50-nm Au nanoparticles (Structure Probe, Inc., product no. 04801-AB). In this case, the demonstrated nanoscale patterning is of high fidelity, and the achieved resolution is on the order of 50 nm. In all the cases presented here, multilength-scale, plasma-induced chemical lithography via PDMS stamps was performing without applying any external pressure (contact was simply made by gravitation); thus, stamp wearing and deformation are not significant issues. We have tested that these PDMS stamps can be used multiple times without degradation.

Dependence on the Plasma Exposure Duration in μCFP Surface Treatment. Figure 3 shows the temporal behavior of plasma diffusion in a PDMS microchannel stamp with a channel width of 20 μm. This PDMS stamps consists of two plasma inlets from both sides of a long channel, and two entering plasma streams meet in the middle of the stamp. Using this specific PDMS stamp and plasma process conditions, for a short duration of μCFP plasma treatment (3 min), the plasma-modified region (darker region in the FE-SEM image) did not reach the center part. In addition, the imaging contrast in the plasma-modified region appeared to have a gradient distribution. By contrast, for a sufficiently long exposure duration (10 min), the channel

(45) (a) Liao, J.-D.; Wang, M.-C.; Weng, C.-C.; Klauser, R.; Frey, S.; Zharnikov, M.; Grunze, M. *J. Phys. Chem. B* **2002**, *106*, 77. (b) Weng, C.-C.; Liao, J.-D.; Wu, Y.-T.; Wang, M.-C.; Klauser, R.; Zharnikov, M. *J. Phys. Chem. B* **2006**, *110*, 12523.
(46) Tatoulian, M.; Bouloussa, O.; Morire, F.; Arefi-Khonsari, F.; Amouroux, J.; Rondelez, F. *Langmuir* **2004**, *20*, 10481.
(47) Schmalenberg, K. E.; Buettner, H. M.; Uhrich, K. E. *Biomaterials* **2004**, *25*, 1851.
(48) West, J.; Michels, A.; Kittel, S.; Jacob, P.; Franzke, J. *Lab Chip* **2007**, *7*, 981.
(49) Lahav, M.; Narovlyansky, M.; Winkleman, A.; Perez-Castillejos, R.; Weiss, E. A.; Whitesides, G. M. *Adv. Mater.* **2006**, *18*, 3174.
(50) Saito, N.; Wu, Y.; Hayashi, K.; Sugimura, H.; Takai, O. *J. Phys. Chem. B* **2003**, *107*, 664.
(51) Srinivasan, C.; Mullen, T. J.; Hohman, J. N.; Anderson, M. E.; Dameron, A. A.; Andrews, A. M.; Dickey, E. C.; Horn, M. W.; Weiss, P. S. *ACS Nano* **2007**, *1*, 191.

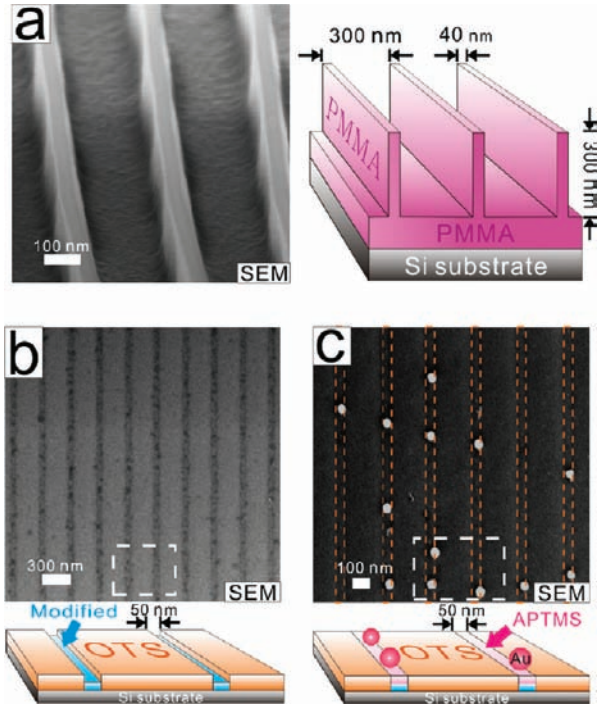

Figure 2. (a) FE-SEM image of a hardened PMMA structure fabricated by electron-beam lithography. This structure was used as a mold to replicate a nanoscale PDMS channel stamp. (b) FE-SEM image of the modified surface using a PDMS nanochannel stamp with a channel width of 50 nm. The imaging contrast is the same as that shown in Figure 1. (c) Using this technique, selective grafting of APTMS and adsorption of Au nanoparticles (50 nm in diameter) can be performed with a high spatial resolution.

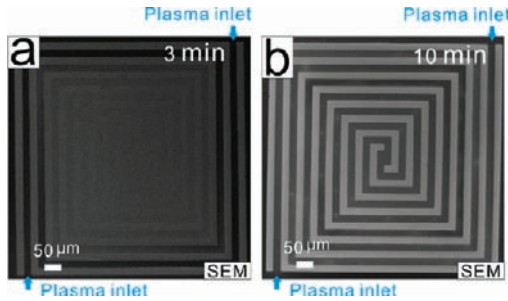

Figure 3. FE-SEM images. (a) Incomplete modification of the OTS monolayer with a short duration (3 min) of μCFP treatment. (b) Complete modification of the OTS monolayer with a sufficient exposure time (10 min).

region was uniformly converted with a constant contrast. This indicates the requirement of an adequate plasma exposure time for μCFP-induced surface modifications and a self-limiting behavior in the terminal surface state.

SEM and SKPM Microscopic Analysis of a μCFP-Patterned Surface. For consistency, we utilized the same "maze"-shaped PDMS stamp with a channel width of 5 μm for all three types (SEM, SKPM, and SPEM) of microscopic analysis. Figure 4a shows the schematic diagram showing the surface condition after μCFP treatment. In Figure 4b and 4c, we show both SEM and SKPM images of a patterned OTS surface after μCFP treatment for 3 min. For this specific PDMS stamp, a plasma exposure time of 3 min is sufficient to reach a terminally uniform image contrast on the modified region. Using SKPM, quantitative measurements of surface potential differences can also be performed and will be discussed later (Figure 8). Here, by using the results from two kinds of microscopic analysis, we can

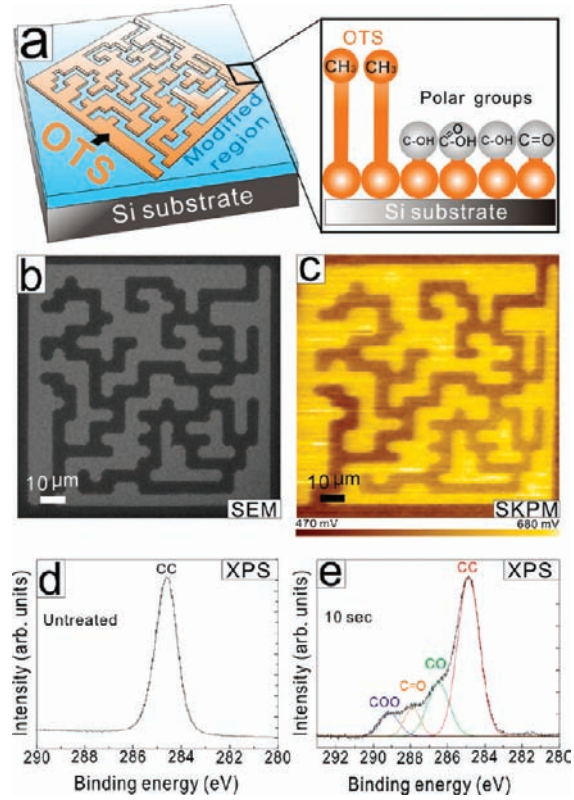

Figure 4. (a) Schematic diagram showing the surface condition after the μCFP treatment. (b) FE-SEM and SKPM image analysis of μCFP surface treatment process. After μCFP treatment for 3 min, an FE-SEM image composed of selectively modified OTS region (darker region) and unmodified OTS region (brighter region). (c) After μCFP treatment (3 min), a surface potential (SKPM) image of selectively modified OTS region (darker region) and unmodified OTS (brighter region). (d) XPS C1*s* signal of an unmodified OTS monolayer. It originates from the C−C bond. (e) XPS C1*s* signal of a modified OTS monolayer after plasma exposure for 10 s. There are three types of plasma-induced carbon bonds, involving surface functional groups of hydroxyl (−OH), aldehyde (−CHO), and carboxyl (−COOH).

confirm that both homogeneous surface conversion and high-fidelity pattern transfer can be achieved in μCFP-based chemical lithography.

XPS and SPEM Characterization. To understand the chemical conversion mechanism of air-plasma-induced surface modification, a synchrotron-based XPS study was performed. From the XPS measurements of unexposed and plasma-exposed OTS monolayers, the chemical conversion mechanism of the plasma-modified OTS monolayer can be attributed to surface hyodroxylation of the terminal methyl groups and sequential oxidation of the resulting hydroxyl groups. As shown in Figure 4d and 4e, while the C 1*s* peak at the binding energy of 284.6 eV originating from the C−C bond is clearly observed for the untreated OTS monolayer, the surface groups on the plasma-modified OTS monolayer were converted into multiple C 1*s* spectral features related to the hydroxyl group (C−O) at 286.5 eV (fwhm: 1.4 eV), the aldehyde group (C═O) at 287.9 eV (fwhm: 1.0 eV), and the carboxyl group (O═C−O) at 289.1 eV (fwhm: 1.2 eV). Additionally, using the bulk Si 2*p* core level as a reference, we have found that the C 1*s* peak originating from the C−C bond shifted to 284.9 eV after plasma treatment. These C 1*s* spectral features are consistent with surface hyodroxylation and sequential oxidation by active oxygen species such as ozone, atomic oxygen, and other oxygen-derived long-living free radicals or metastable species. In our process,

these active oxygen species are likely derived from the plasma excitation of oxygen molecules in air.[45]

In Figure 4e, the peak intensity (I) ratio measured on the plasma-modified region was found to be 1:1.3:2.4:7 ($I_{COO}/I_{C=O}/I_{CO}/I_{CC}$). For an ideal OTS monolayer, using our XPS probing geometry (escape angle of 60° with respect to the surface normal), the XPS signal from the topmost carbon atoms compared to that from the rest of carbon atoms can estimated to be ca. 1:3. Apparently, the plasma treatment also causes the shortening of the alkyl chain length if we consider all of the modified carbon groups originate from the topmost methyl groups (therefore, the measured ratio is 5:7 instead of 1:3). In a recent work reported by Kim et al., a similar alkyl chain etching phenomenon was also reported for VUV-light-induced photooxidation of *n*-octadecyltrimethoxysilane self-assembled monolayers in air (VUV light wavelength: 172 nm).[14] In addition, the induced C 1*s* spectral features revealed by them are quite similar to our case, indicating a similar surface modification mechanism in both cases.

We have also applied the SPEM technique to visualize the lateral distribution of μCFP-patterned regions with a channel width of 5 μm. The SPEM technique allows chemical mapping of different elements or the same element with different chemical environments. Figure 5a and 5b show chemical mapping images at two different binding energy ranges of C 1*s* emissions, corresponding to the C—C bond in the unmodified OTS region and the C—O, C═O, and O═C—O bonds in the plasma-modified region after μCFP treatment for 3 min. It can be clearly seen that in the SPEM image the plasma-modified region is tightly confined within the microchannel region. In addition, after prolonged exposure of air plasma, the surface function groups remain to be oxidized carbon-containing species although most of the alkyl chains might have been completely etched.

To gain a better understanding of the etching process of the alkyl chain implied by XPS peak intensity analysis [Figure 4e], we have measured the C—C 1*s* core-level peak at 284.9 eV as a function of plasma exposure time. From the decay behavior of the C—C 1*s* core-level peak with increasing plasma exposure time [Figure 5c], we can confirm that this plasma treatment not only converts the surface functional groups but also etches the alkyl chain of OTS molecules. The exact OTS monolayer thicknesses after plasma treatment with different exposure times were measured by AFM on Si surfaces covered with OTS monolayer islands. The AFM images show that the OTS islands were etched uniformly in a "digital" fashion [Figure 5d]. The measured etching rate is ca. 1.5 s per CH_2 length. After ca. 25 s of plasma exposure, the alkyl chain is shortened to the siloxane headgroup and this etching process abruptly stops. Determined by the AFM-based OTS height analysis, the terminal thickness of plasma-modified OTS is ca. 0.4 nm, which roughly corresponds to the total length of the anchoring head and modified surface groups of OTS molecules. Since the head groups of organosilane molecules form a strong −Si−O−Si-O− bonding network with the Si substrate, the OTS/Si interface is mostly intact in the plasma etching process, unlike the plasma treatment case of alkanethiolate SAMs on Au.[45]

Grafting of APTMS and Adsorption of AuNPs onto a μCFP-Patterned "Maze" Surface. After μCFP treatment, the patterned region can be oxidized by the air plasma. As a result, the patterned surface becomes hydrophilic and terminated by the hydroxyl groups, which can allow subsequent grafting of APTMS monolayers. Under a suitable pH condition in a gold colloidal solution, the APTMSs are protonated (positively charged with NH_3^+ functional groups) and can be used to selectively adsorb negatively charged colloidal AuNPs.[27,29] Figures 6 and 7 show FE-SEM and SKPM images after grafting of APTMS and adsorption of AuNPs onto a μCFP-patterned "maze" surface. These images show that, using our approach, excellent surface homogeneity can be achieved for both APTMS grafting and AuNPs adsorption.

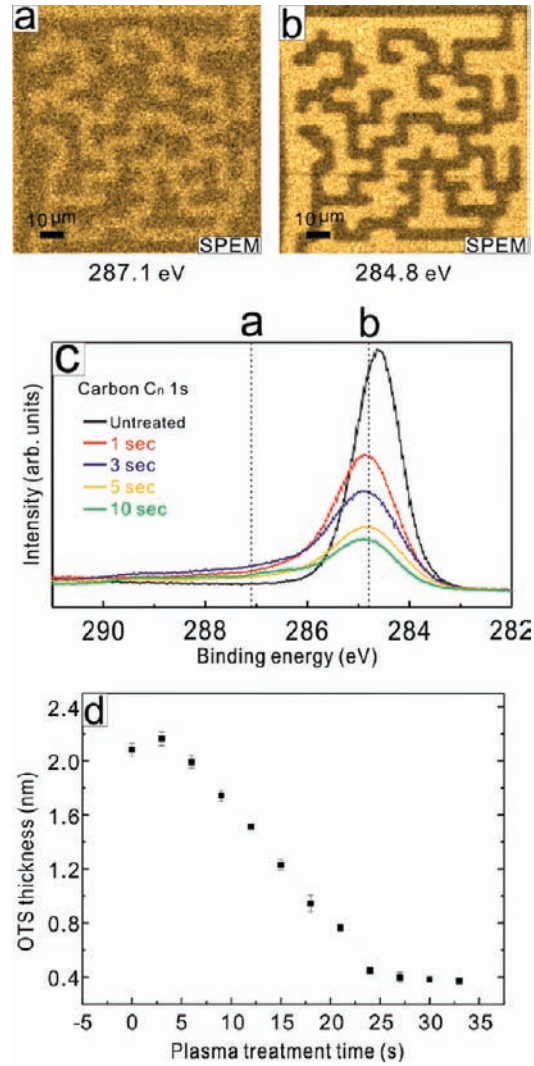

Figure 5. SPEM image analysis of the μCFP surface treatment process. (a and b) SPEM images of a plasma-modified region after 3 min of μCFP treatment. (a) In the binding energy window centered at 287.1 eV (window size: 0.75 eV), which corresponds to the C—O and C═O bonds. (b) In the binding energy window centered at 284.8 eV (window size: 0.75 eV), which mainly corresponds to the C—C bond. (c) XPS spectra after plasma treatment for 1, 3, 5, and 10 s. (d) The plot of the OTS island thickness measured by AFM versus the plasma treatment time, showing the behavior of "digital" etching of the alkyl chain.

Surface Potential Measurements. In recent years, SKPM has been demonstrated as a powerful tool for detailed characterization of surface potential distribution on patterned self-assembled monolayers with nanoscale resolution. Especially, the surface potential contrast between polar and nonpolar terminal functional groups and between different polar groups can be directly measured, which can provide valuable information on the orientation/magnitude of the surface dipole moments as well as molecular ordering, length, and packing density.[52,53] There-

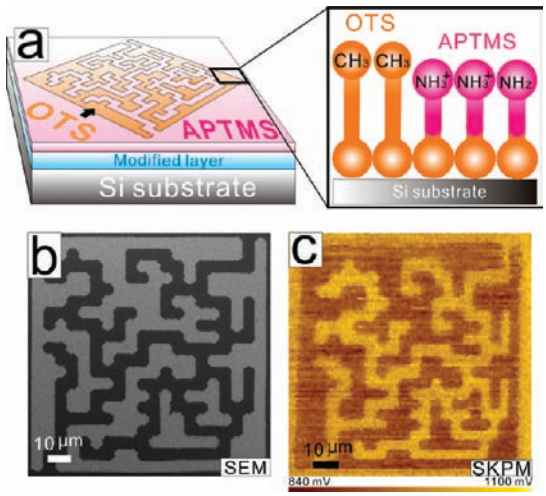

Figure 6. SKPM image analysis of selective grafting of APTMS onto a μCFP-patterned surface. (a) Schematic diagram illustrating APTMS grafting onto a modified OTS monolayer region. (b) FE-SEM image of a selectively modified region composed of an APTMS-grafted region (darker region) and an unmodified OTS (brighter region). (c) Surface potential (SKPM) image of a selectively modified region composed of an APTMS-grafted region (brighter region) and an unmodified OTS (darker region).

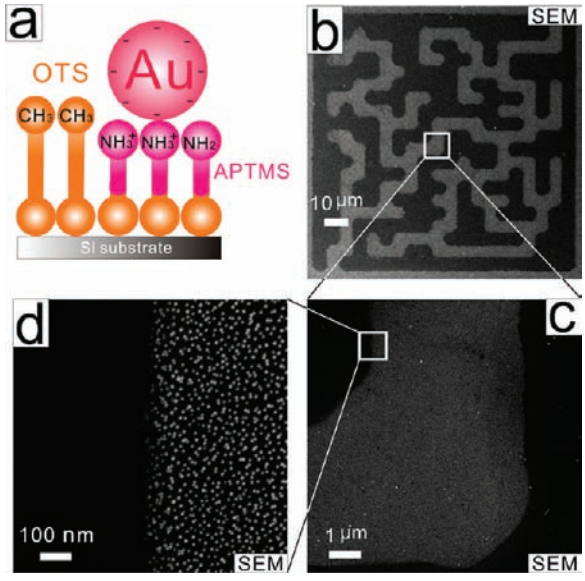

Figure 7. FE-SEM image analysis of selective adsorption of Au nanoparticles onto a μCFP-patterned and APTMS-grafted surface. (a) Schematic diagram illustrating selective adsorption of Au nanoparticles onto the APTMS-grafted region. (b−d) Three FE-SEM images (different magnifications) of a selective adsorbed area, composed of both Au nanoparticles and unmodified OTS regions.

fore, information complementary to the XPS analysis can be obtained by SKPM.

On the μCFP-patterned regions of modified/OTS, APTMS/OTS, and AuNPs/OTS, we can measure their surface potentials of the polar regions with respect to the unmodified, methyl-terminated OTS region. In Figure 8, the acquired surface potential contrast of the modified/OTS region is −90 meV, while that for the APTMS/OTS region is +120 meV. These results

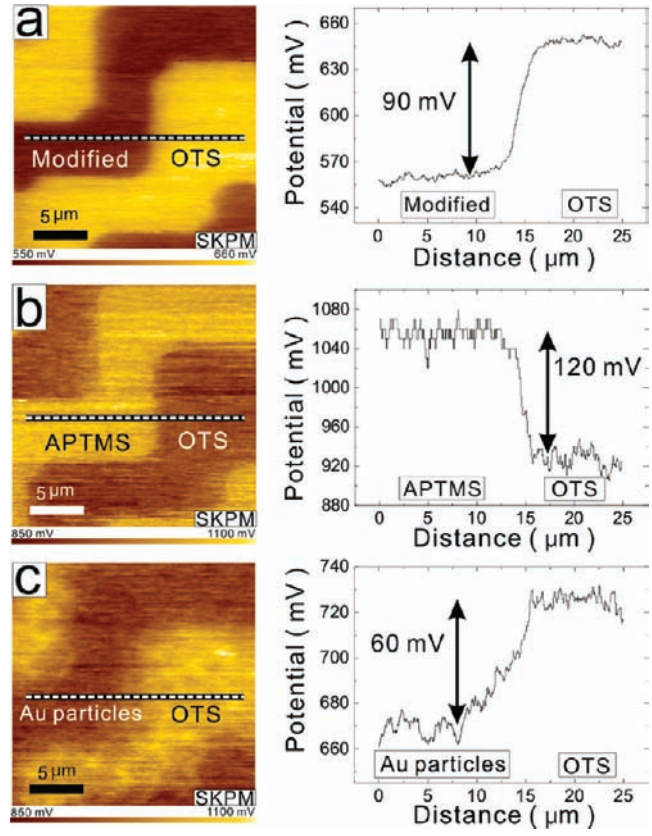

Figure 8. Surface potential measurement. (a) SKPM image of μCFP-patterned (3-min plasma exposure) OTS surface composed of hydroxyl- and OTS-covered regions. (b) SKPM image of μCFP-patterned surface composed of APTMS- and OTS-covered regions. (c) SKPM image of μCFP-patterned surface composed of AuNPs- and OTS- regions.

are in agreement with the expected surface dipoles of respective functional groups on these regions. Interestingly, the potential contrast observed for the AuNPs/OTS region is −60 meV despite that AuNPs are selectively adsorbed onto the APTMS-covered region. This observation is actually consistent with the fact that gold colloidal particles suspended in water are negatively charged. The large potential contrasts measured by SKPM indicate that high chemical selectivity and good monolayer quality (first and second monolayers) can be achieved on the μCFP-patterned OTS/Si surface.

Conclusions

We have shown that μCFP-based chemical lithography can be efficiently applied to pattern SAM surfaces with designated surface functionalities. Using a complete set of characterization tools, we have confirmed the capability of multilength-scale chemical patterning with feature sizes ranging from nanometer to centimeter. In addition, the detailed conversion mechanism by air plasma has been elucidated. We provide convincing evidence that the plasma-induced oxidation and etching is limited to the carbon chain of OTS-SAM. The self-limiting nature of the plasma modification process is very critical to achieve exquisite spatial resolution by avoiding the strong interaction of plasma with the substrate. The patterned SAMs demonstrated here can be widely used as surface templates for hierarchical organization of single nanoscale objects such as molecules and nanoparticles. This method, due to its advantages of scalability, parallel processing, and general applicability, could open up a practical approach to interface nanoscopic devices and structures with the macroscopic world.

(52) Sugimura, H.; Hayashi, K.; Saito, N.; Nakagiri, N.; Takai, O. *Appl. Surf. Sci.* **2002**, *188*, 403.
(53) Ichii, T.; Kukuma, T.; Kobayashi, K.; Yamada, H.; Matsushige, K. *Nanotechnology* **2004**, *15*, S30.

Acknowledgment. This work was funded by the National Science Council in Taiwan through the National Nanoscience and Nanotechnology Program (NSC 97-2120-M-007-005) and the Foresight Taiwan Project (NSC 98-3011-P-007-001).

Supporting Information Available: In the Supporting Information, we demonstrate the importance of a predeposited OTS-SAM with a self-limiting nature while interacting with the air plasma. Six figures are included in this file: Channel-mediated plasma modification of a 500-nm-thick PMMA film without the use of a self-limiting SAM while interacting with the air plasma (optical images) (Figure S1); Channel-mediated plasma modification of a 500-nm-thick PMMA film without the use of a self-limiting SAM while interacting with the air plasma (FE-SEM image) (Figure S2); Schematic illustration of channel-mediated vapor deposition of a patterned SAM (Figure S3); Boundary effects of microchannels in channel-mediated vapor deposition of a patterned SAM (Figure S4); Residual PDMS pattern created by physical contact of the PDMS stamp with a surface which is not covered by a SAM layer (Figure S5); Uniform and smooth chemical modification of OTS-covered surafce via channel-mediated plasma modification (Figure S6). This information is available free of charge via the Internet at http://pubs.acs.org.

JA901619H